water

MDPI

Article

Analysis of the Role of Aquatic Gases in the Formation of Sea-Ice Porosity

Vadim K. Goncharov [1,*] and Natalia Yu. Klementieva [2]

[1] Faculty of Shipbuilding and Ocean Engineering, Department Ocean Engineering and Marine Technologies, Saint Petersburg State Marine Technical University, Saint Petersburg 190121, Russia
[2] Krylov State Research Centre, Saint Petersburg 196158, Russia; nuklem@mail.ru
* Correspondence: vkgonch@mail.ru

Abstract: The porosity of freshwater ice and sea ice is one of the main parameters that determine their strength. The strength of ice varies over a wide range of values, and the differences in the intensity of the mechanisms of ice porosity formation in different water areas can be one of the possible reasons for these variations. The water mass contains gases in two forms: gases dissolved in the water mass, as well as gas bubbles that are formed when wind waves break up, and bubbles that float up from the seabed. This article presents the results of an analysis of the role of each of these forms in the formation of gas inclusions (pores) in the crystal structure of ice. The results showed that the main source of gas pores in ice crystals is the gas bubbles coming to the surface from the bottom, formed during the decomposition of bottom sediments or during gas leaks from near-bottom oil and gas fields. The possibility of gas bubbles occurring and rising to the ice–water boundary depends on the presence of bottom sources of the gases, the intensity of dissolution of the bubbles and the depth of the water area. Therefore, the variation in the porosity and the strength of ice over the space of the water areas can be associated with the changes in their depths, and the presence and location of the natural gas sources.

Keywords: ice; crystal; porosity; bubble; gas; dissolution; emerging; water

Citation: Goncharov, V.K.; Klementieva, N.Y. Analysis of the Role of Aquatic Gases in the Formation of Sea-Ice Porosity. *Water* **2024**, *16*, 2213. https://doi.org/10.3390/w16152213

Academic Editors: Em. Ove Tobias Gudmestad, Zhijun Li, Li Zhou and Sasan Tavakoli

Received: 25 June 2024
Revised: 29 July 2024
Accepted: 30 July 2024
Published: 5 August 2024

1. Introduction

The surface water mass in seas and oceans is influenced by processes in the atmosphere and at depth, the intensity of which varies over time. Therefore, all processes occurring on the sea's surface are non-stationary. In order to study any of these processes, it is necessary to assume the negligible influence of other processes occurring in the water mass. In the problem under consideration, the formation of the ice cover and its structure, as well as the absence of current and wind waves, is assumed. This implies the formation and growth of ice crystals on the surface of a stationary water mass, in which only thermoconvective vertical currents occur.

The ice cover on the surface of the freezing seas has a crystalline structure that differs significantly from the crystalline structure of freshwater ice on rivers and lakes. This difference is primarily related to the conditions of the ice-cover formation and the salinity of the seawater.

Freshwater ice crystals are formed in the cooling horizontal layers of water, which have a lower density at freezing temperature (compared to the maximum at +3.98 °C), and take the form of horizontal plates with a vertically directed optical axis.

Sea ice crystals arise under conditions of the constant vertical convective upward–downward movement of cooling on the boundary surface (ice–water interface) and therefore become heavier than sea water. Therefore, they have the form of vertical plates with a horizontal optical axis. Subsequently, the crystal structure of the sea ice is affected by changing meteorological conditions, as well as the interaction of ice floes with each other

under the influence of the wind, waves and currents. As a result, sea ice has up to nine types of crystalline structure [1–3], differing in size, shape and the orientation of the crystals.

During sea-ice formation, the brine drops (solution of salts with high concentration) and gas cavities appear among its crystals, which form the specific characteristic property—ice porosity. The shape and size of the ice crystals, as well as the value of the porosity, determine the mechanical properties of the sea ice [1,4]. Therefore, they are the subject of special investigations in the interests of assessing the loads on offshore structures and the ice propulsion of ice-going ships. The content of the brine and gas cavities also determines the specific properties of the sea-ice cover, which are manifested during microwave sounding [5,6]. In addition, there are reasons to believe that the composition of the gas cavities contain some information about the conditions for the formation of sea ice, and this information can have many practical applications.

The effects associated with the presence of microscopic gas inclusions (bubbles) in the structure of ice of various natures, and manifested in variations in the strength characteristics of ice, have been studied in relation to many practical problems [7–9]. This confirms the relevance of experimental and theoretical studies of the processes of formation of gas inclusions in the crystal structure of ice.

This article contains an analysis of the possible mechanisms of sea-ice saturation with gas cavities, including:

- The displacement of the air dissolved in the seawater during crystallization;
- The replacement of heavy brine flowing down with atmospheric air;
- The penetration of gas bubbles contained in the water space and emerging from the seabed sediments into the crystal structure of the sea ice.

The results of the analysis of the available experimental data of the porosity of sea ice are presented in order to assess the comparative reality of the mechanisms of the gas-pore formation under consideration. For the same purpose, computer modeling of the processes of gas inflow to the ice–water ice-forming boundary was carried out.

The study provided grounds for the conclusion that the main source of the gas pores in sea ice are gas bubbles emerging from the seabed.

The conclusion presents the main results of the studies and recommendations for further research and practical applications.

The preliminary results of the problem studies were presented in part at the International Scientific Conference POAC 2011 [10].

The purpose of this article is to provide a more detailed presentation of the methodology and results of the mathematical modeling of the processes of saturation of sea ice with gas bubbles. This will improve the understanding of the reasons for the variation in ice strength over the sea area, and provide the basis for using ice porosity characteristics to search for near-bottom sources of natural gas.

2. Porosity of Sea Ice and the Main Peculiarities of Gas Cavities

Sea-ice porosity is one of the main characteristics that determine the strength of ice, and it is therefore the object of study using various methods. Microphotography is the most informative method because it allows the isolation and analysis of the parameters of individual gas cavities. Figure 1 presents an image of the microstructure of first-year congelation of ice under a temperature of −15 °C (image width is 3.5 mm) [11].

The form of sea-ice porosity with the specified gas cavities differs significantly from that of freshwater ice. While the gas cavities in freshwater ice have a form close to spherical [9], the gas cavities in the sea ice have a variety of forms. There are cavities with forms close to spherical, elongated cavities and channels of varying heights, as presented in Figure 1 (sea ice also contains pockets of brine—a strong salt solution that is black in colour.). This variety of gas cavity form gives us reason to consider that there are various mechanisms involved in the formation of gas cavities in sea-ice formation.

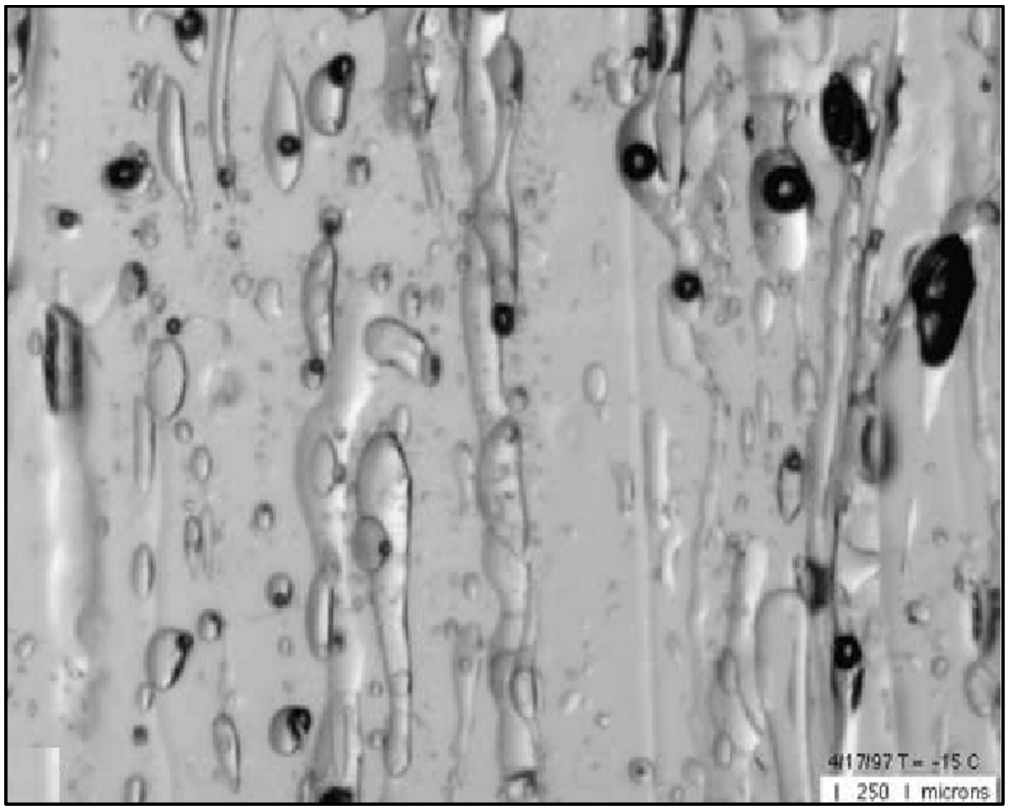

Figure 1. Porosity of a sea-ice sample. The light-coloured pockets are the gas cavities with different forms and the black-coloured pockets are the brine drops (imported from [11]).

3. Possible Mechanisms for the Formation of Gas Cavities in Sea Ice

The initial stage of the ice-cover formation is the stable hexagonal ice crystals initiation from the initially unstable and near-tetrahedral internal structure of liquid water. The main regularity of the formation of stable ice crystals is the minimization of the internal energy of the crystal lattice, which causes the displacement of foreign substances—impurities from the initial solution, which are the salts and gases contained in the seawater [12–14].

Unlike the salts, the gas molecules do not chemically connect with the polarized water molecules. The gas molecules locate in the space within the liquid water crystals. Therefore, the solubility of the gases in the water space increases with the pressure and decreases when increasing the temperature, which leads to the destruction of the water crystals. The seawater is in constant dynamic interaction with the atmosphere, therefore its surface layer contains the limiting–saturating concentration of the dissolved air and bubbles that occur when the wind waves break. The concentration of dissolved gases increases with increasing depth [15], and the content of the dispersed gas bubbles decreases [16].

During ice-crystal formation, the excess air (contained in the deep-water mass rising with the convective current to the zone of ice formation) displaces at the ice–water interface. The main part of this air forms bubbles, which are captured and then frozen into the space between the ice crystals. The cavities of near-spherical form visible in Figure 1 are the most likely outcomes of this mechanism.

Gas bubbles formed when wind waves break up appear only near the boundaries of the ice cover, which is an obstacle to wave movement. Therefore, this source of gas bubbles makes a negligible contribution to the gas porosity of the sea ice.

Another possible mechanism for sea-ice saturation with gas cavities is the penetration of the atmospheric air into channels that remain in the upper layer of the ice cover behind the sea's salt water flowing down between the ice crystals. This process takes place under the gravity's action on the salt water while the ice cover is freezing and its thickness increases due to the rise of its surface above the sea level [5]. During the ice-crystal

formation, the molecules of salts dissolved in the water are displaced into the water-filled spaces between the ice crystals, increasing the concentration of the salts and forming the brine drops. The volume and salinity of the brine varies under the action of the temperature variation due to the formation or the breaking of the chemical bonds between the salt and water molecules, and therefore the cavities are filled with the brine and the air together. These air-filled vertical channels of various lengths (heights) and thicknesses, and the cavities with brine and air together, are observed in Figure 1.

It is possible that the third mechanism of sea-ice saturation with gas cavities is not related to the crystallization of the seawater. At the ice–water interface, gas bubbles can float up from the bottom sediments, where the decomposition of organic matter deposited on the bottom occurs (this option is the most significant for the shallow coastal water areas). In the water areas with bottom deposits of natural gas, methane can seep into the water space and form bubble plumes which rise from great depths to the ice cover [17]. The gas bubbles reaching the ice–water interface have dimensions exceeding those formed during the crystallization and displacement of the air dissolved in the seawater. Therefore, these bubbles can be assumed to be the elongated gas cavities in Figure 1 and related to this possible mechanism.

To assess the reality and the role of these mechanisms in the formation of the physical and mechanical properties of the sea ice, it is necessary to analyse the available experimental data on measuring the porosity of sea ice and numerically simulate the processes of the gas bubbles' movement to the sea water–ice interface.

4. Analysis of Experimental Data

Investigation of the gas cavities in fresh-water ice and sea ice is a very complicated problem because it requires special devices for registering the dimensions and form of the small gas cavities, and equipment for the temperature of the ice sample stabilization.

In many publications devoted to the research of the physical and mechanical properties of sea ice, the integrated estimations of the total porosity of the air-bubble and brine-drop contents are stated. In the data [5], the porosity lies in a range of 20–60‰, and also has the greatest value near to the lower surface of the ice cover where it reaches 200‰. In [1], it was stated that sea ice has a porosity in a range of 1–50‰. Porosity has a maximum value of 12–18‰ in the top and lower layers of the young ice, and a minimum of 8‰ in the centre layer. According to [18,19], the air bubbles are dispersed in all ice thickness, but the greatest concentration of the gas bubbles was observed near to the top surface of the ice.

The dynamics of brine inclusions in first-year sea ice formed the main content of the investigation presented in [11]. The characteristics of the gas cavities of near-spherical form (bubbles) were also analysed, and the following results were obtained. The gas bubbles had a radius in a range of 0.004 mm to 0.07 mm. Their total density was 1.3 per mm^3.

According to the results of the measurements performed in the samples from the top layer of the first-year ice (named "bubbly" ice) [20], the bubble radii were in the range of 0.2–2 mm and their number per mm^3 was in the range of 0.004 (largest bubbles)–0.09 (smallest bubbles).

Detailed investigations of the total air content in the sea ice was performed in [19], where the vertical distribution of the density, the salinity and the porosity (air content only) sampled in Baffin Bay was measured in two cores of the first-year ice in a diameter of 75 mm. The first core had a length of 0.740 m and was investigated in situ. Samples—pieces with a thickness of 50 mm—were cut, and each sample was controlled apart. The second core, 0.795 m in length, had been frozen to −40 °C and delivered to the laboratory, then investigated with a discreteness of 25 mm. Arrays of the sea-ice characteristics were obtained: core No. 1–15 values and core No. 2–32 values. This method allowed us to get a more detailed understanding of the considered phenomenon and to draw statistically significant conclusions. Table 1 contains the averages (length of the cores averaged-out) and dispersions of the density, the salinity and the porosity of the ice for each core and for its unified array.

Table 1. Statistical characteristics of the sea-ice properties [19].

Sea-Ice Property		Core No. 1	Core No. 2	Unified Array
Density, g/cm^3	average	0.911	0.913	0.912
	dispersion	7.533×10^{-5}	8.097×10^{-5}	7.981×10^{-5}
Salinity, ‰	average	3.458	3.633	3.577
	dispersion	1.682	2.395	2.133
Porosity, %	average	1.246	1.090	1.140
	dispersion	1.193	1.336	1.269

Comparison of the measured values of the sea properties—density, salinity and porosity (average of the height of each core)—using "Student criterion" revealed that the difference between the cores is not statistically significant. It means an essential change in characteristics of the No. 2 core during transportation and storage did not occur (the probability of observing a similar or smaller difference between these characteristics of the sea ice for any other cores from the same ice field equalled 50–70%). This allowed us to analyse the data from both cores as a unified array of 47 volume values for each characteristic.

Figure 3 presents the variation of porosity (on the left) and salinity (on the right) along the cores (on thickness of ice). The analysis of this data shows the following:

1. The obvious similarity of the porosity and salinity variation along the length of the cores;
2. The similarity of the porosity and salinity variation along both cores;
3. The substantial increase in the porosity and salinity values on the upper and lower boundaries of the cores, and the rather small variation in these parameters in the middle parts of the cores;
4. Variation of the porosity as random quantity fits the Weibull probability density function, presented in Figure 2.

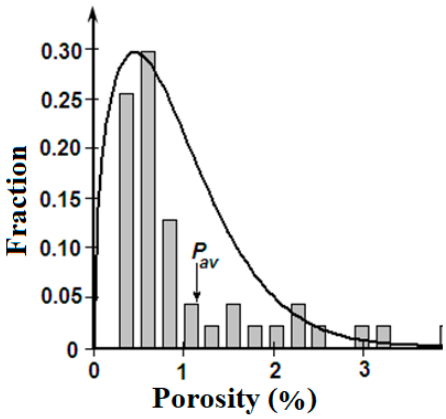

Figure 2. Histogram of porosity for unified sample and Weibull probability density function.

Higher salinity in the upper and lower layers of the first-year sea ice was marked in much of the research [1,18]. The phenomenon of porosity increase in the border layers of the sea ice requires special investigation.

The correlation analysis between measured characteristics of the sea-ice density, salinity and porosity, based on the unified array of their values, was carried out. Table 2 presents the results of the coefficients of correlation estimations.

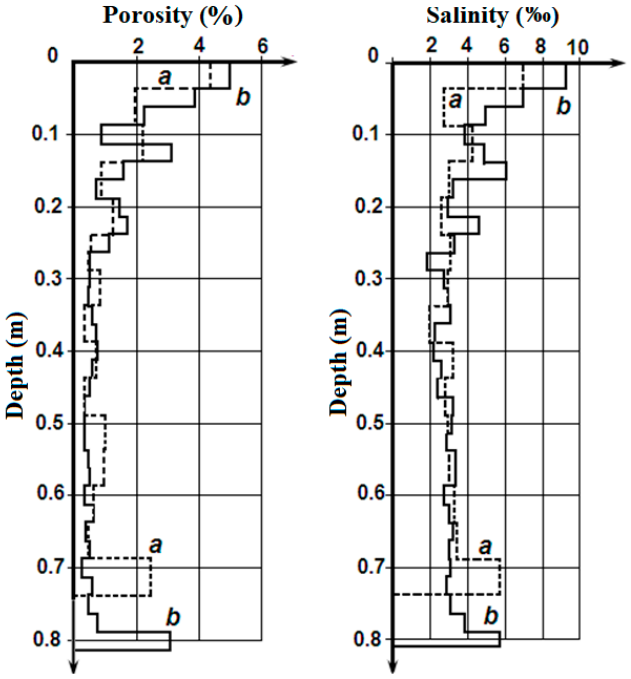

Figure 3. Variation of the sea-ice porosity (on **left**) and the salinity (on **right**) along ice cores No. 1 (*a*) and No. 2 (*b*) [19].

Table 2. Correlation between characteristics of the sea ice.

Characteristic	Density	Salinity	Porosity
Density	X	−0.834	−0.965
Salinity	−0.834	X	0.892
Porosity	−0.965	0.892	X

All values of the correlation coefficients are great enough, and it is possible to consider them as statistically significant values. The analysis of Table 2's data allows us to form the following conclusions:

1. A high correlation between the sea-ice density and porosity is natural and does not demand additional comments.
2. A high, but negative, correlation between salinity and density seems strange. However, the average value of salinity S_{av} = 3.577‰ is essentially less than the average value of the porosity P_{av} = 1.140%. Therefore, the contribution of the porosity to the density of the sea ice is more than the contribution of the salinity. The negative sign of the correlation, salinity—density, is in this case connected to porosity.
3. A high and positive correlation between the porosity and the salinity of the sea ice requires special investigation.

Figure 4 presents a linear regression of porosity on salinity. These results show that a high correlation between porosity and salinity is connected to the largest values of these parameters, which amounts, approximately, to 1/5 part of an array. The main bulk of data are grouped in the minor area—$S < 4$‰ and $P < 1$%— where any statistically significant interdependence between porosity and salinity is difficultly to establish.

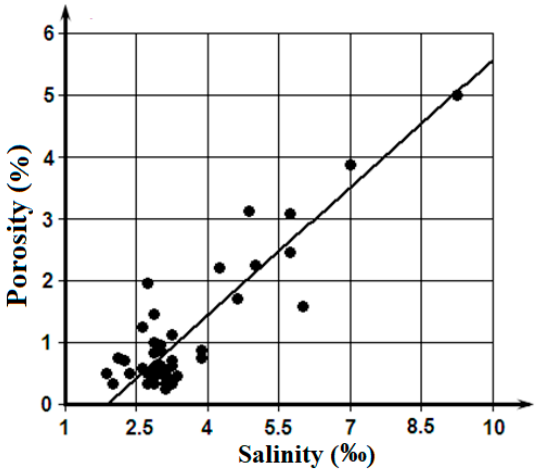

Figure 4. Linear regression of the sea ice porosity on it salinity for the integrated samples.

It is reasonable to apply the presented outcomes of the accessible experimental data analysis of the possible mechanism of the sea-ice crystalline structure to the gas bubble-saturation analysis.

5. Evaluation and Modelling of the Mechanisms of Sea Ice with Gas-Bubble Saturation

5.1. Displacement of the Dissolved Atmospheric Air and Capturing the Bubbles Contained in the Seawater

The main and evident mechanism of sea-ice saturation with atmospheric air is the displacement of the seawater before the air is dissolved into bubbles during the course of formation and growth of the ice crystals. According to [15], in the waters of the Northern Atlantic (for example), the content of the basic components of the atmospheric air are as follows: nitrogen 9.2–14.4 mL/L and oxygen 6.99 mL/L. Therefore, the average content of air dissolved in the seawater is 16.2–21.4 mL/L. Taking into account the increase in volume of the ice in comparison with the volume of the unfrozen water, it is possible to accept that the volume of the air in the ice will be 14.85–19.62‰. These values exceed porosity in the central part of the cores [19], which confirms the effect of displacement of the atmospheric gases at the ice crystallization. At the same time, porosity in the lower layers of the cores that turned into water space considerably exceeds the specified values.

The zone of contact: ice–water space is the area of their continuous interaction. Therefore, characteristics of ice and water in this zone considerably differ from other volumes of ice and water [21]. It is possible to expect that the crystal structure of the sea ice in the bottom layer is less compact than in the overlying layers. Hence, this layer is capable of containing a larger quantity of gas bubbles in the case of its inflow from the water column. The drops of "brine" gradually flow down to the same layer from overlying ice layers, and these can explain the correlation of porosity and salinity in the bottom layers of both cores [19].

To evaluate the reality of the indicated mechanism, it is necessary to examine the following sources of bubbles. Air bubbles appear in the near-surface layers of the sea owing to the breaking-down of wind waves and as result of other (including biological) processes. The wind waves are absent in the presence of the ice cover of the sea surface. Therefore, it is necessary to pay attention to the bubbles of various origins that have existed for a long time in the water space owing to the organic film of surfactants preventing their dissolution.

Results of research, using various methods [16,22], on the content of the air bubbles in the near-surface layer of the seas has shown the bubbles with radii in a range of 2.5–20 microns existing at depths greater than 5 m. Their volume concentration was in a range from 1300 to 25 L/m^3, accordingly. Based on these data, it is possible to estimate a flux of the air from the water column on the lower surface of the ice cover.

As stated in [16], the average rate of the sea–ice growth was about ≈0.05 micron/s. It is possible to assume that the bottom layer of the cores of a 50 mm thickness freeze to some extent in about 278 h. The velocity of the air bubbles floating up (if representing them in the form of a sphere and applying Stokes equation [23]) can be estimated using the following formula:

$$w = \frac{2\,g\,R^2}{9\,\nu}. \quad (1)$$

In this formula, g—the gravity acceleration (9.81 m/s^2), ν—the kinematic viscosity of the seawater (1.826×10^{-6} m^2/s for 0 °C and 34.3‰) and R—the radius of the air bubble. For the bubble of radius R_1 = 2.5 microns, the velocity of emersion is $w = 7.46 \times 10^{-6}$ m/s, and for the air bubble of radius R_2 = 20 microns, $w = 4.68 \times 10^{-4}$ m/s. The flux of the air from the water space through the area unit (1/m^2·s) can be estimated using the following formula:

$$q = \frac{4\,\pi\,R^3\,w}{3}. \quad (2)$$

The performed calculation showed that the inflow of the air on the bottom surface of the ice cover for the freezing period up to a thickness of 50 mm can achieve the following values: for the bubbles with R_1 = 2.5, microns inflow $Q_1 = 6.40 \times 10^{-7}$ mL/m^2·s, and for the bubbles with R_2 = 20, microns inflow $Q_2 = 4.00 \times 10^{-4}$ mL/m^2·s. These quantities are negligibly small in comparison with the porosity of the ice cores in the lower layer. Therefore, the examined source of the sea-ice saturation with the air does not play an essential role.

5.2. Penetration of the Atmospheric Air into the Channels behind Salt Seawater Flowing Down

The sea-ice density depends on its salinity and porosity, and varies in a range of 0.834 g/cm^3–0.924 g/cm^3. The sea ice that does not contain air has a density of 0.940 g/cm^3 [1], which means that the sea ice is lighter than the water. Therefore, the upper surface of the ice cover rises over the sea-water level. This rise defines the length of the channel that is left after the salt water flows down. The snowfall on the ice cover and freezing close up this channel and new channels form. It is possible to estimate the extreme heights of these channels' dependence on the thickness and density of the sea ice.

The minimal height of the channel appears in the young ice cover, when the upper surface comes up to the water surface. This is the sea ice form named "light nilas" and it has a thickness in the range of 5–10 cm [1].

With regard to the maximal density of the sea ice, the elevation of the ice surface above the water level is 0.3–0.8 cm, and it is the minimal dimension of the air-filled vertical channels between the ice crystals.

It is possible to consider as the maximal dimension of the air channels the thickness of the "first-year" ices in a range of 0.3–1.2 m. During the ice cover summer melting, the "dried ice" contains the through channels, through which melt water flows down.

It is possible to explain the increased porosity in the top layer of the ice cover adjoined to the snow cover by the air replacement of channels, which are formed as a result of the salt water draining to the depth of the ice cover [5]. At the same time, results of measurements of the salinity in the ice cores, presented in Figure 2, do not give a sufficient basis for the analysis of this process, for example, by methods of the theory of filtration as the salinity does not increase, and even decreases in the direction of the middle parts of both ice cores. It is possible to assume that the process of filtration of the salt water has occurred at the early stages of the ice-cover formation, when the temperatures of the atmospheric air and the ice surface were higher than at the time of the sampling of the cores. When the temperatures of the air and the ice surface decrease, this process gradually stopped, and the examined profiles of the salinity and the porosity were generated. This phenomenon requires special research, for example, through a survey of the cores selected at different stages of the ice-cover freezing, using the technique from [19].

5.3. Floating Up of the Gas Bubbles to the Ice–Water Interface

Possible sources of the gas bubbles in the seawater space are the organic bottom sediments in the course of decomposition and the seabed natural gas deposits that release the methane in the form of the bubbles emerging at the sea's surface. Plumes of the bubbles containing methane gas exist in some water areas [24,25].

In the course of floating, the majority of the bubbles are dissolved and, as result, the ocean waters contain the dissolved methane in a concentration of 10^{-3} mL/L in the near-bottom layer and of about 10^{-4} mL/L in the overlying water space [15]. Performed modelling of the bubbles emerging and the dissolution processes for the Okhotsk and the Black Sea [26,27] confirms the reality of these sources.

Methane can play an essential role in the increase in sea-ice porosity in the case when bubbles containing methane are able to emerge from the seabed (and not be completely dissolved) and move to the lower border of an ice cover. The possibility of gas bubble dissolution, in turn, depends on their original sizes and on the depth from which they emerge [26].

Occurrence of the bubbles containing methane from the bottom sediments is most probable at depths of less than 250 m, as at greater depths methane can exist only in methane's crystalline hydrate form. It can be assumed that the ice cores investigated in [19] were most likely taken off the inshore part of the water area.

To estimate the real possibility of methane bubbles coming up to the lower surface of the ice cover, the mathematical model of the floating up and dissolution of a single gas bubble in the sea space [26] was applied.

A feature of this model is that it takes into account the counter-current diffusion of gases: diffusion of methane, which originally filled the bubble in the aqueous medium, and diffusion of nitrogen and oxygen dissolved in the sea water into the bubble.

The flow of nitrogen and oxygen into the bubble partially compensates for the methane dissolved in the surrounding water mass and prolongs the time of existence and height of the bubble surfacing.

To describe the counter-current diffusion of gases, it was necessary to introduce components describing the diffusion of nitrogen and oxygen into the equation of the bubble-diffusion process. Three equations of the mole fractions of methane, nitrogen and oxygen variation were added to the mathematical model.

This model includes the following components:

The equations for the gas-bubble movement that take into account the resistance of the bubble-movement's dependence on its volume and form connected to the dissolution and the external hydrostatical pressure which decrease in the process of floating:

$$\frac{dz}{dt} = w, \quad \frac{dw}{dt} = 2\,g - \frac{3}{4}\zeta\frac{w^2}{r}. \tag{3}$$

The equation for the radius of bubble evolution owing to the diffusion of gases contained in a bubble through its surface and owing to a change in external pressure.

The first two components in curly brackets characterise the variation of the radius of the bubble due to a decrease in external pressure (surfacing), and the third component characterises the variation in the radius of the bubble due to the diffusion of gases:

$$\frac{dr}{dt} = \left\{ \frac{\rho_w\, g\, r\, w}{3} - \frac{r\, w}{3}\left[p_a + \rho_w\, g(H-z) + \frac{2\,\sigma_w}{r} \right] \times \frac{\sum\limits_{j=1}^{3} \rho_{a\,j} \frac{d\kappa_j}{dt}}{\sum\limits_{j=1}^{3} \rho_{a\,j}\, \kappa_j} + \frac{1.45}{\pi}\sqrt{\frac{w}{r}} \sum_{j=1}^{3} \rho_{a\,j}\, \varepsilon_j \sqrt{k\, D_j} \times \right.$$
$$\left. \times \left[\alpha_{w\,j}\, p_a - \left(p_a + \rho_w\, g(H-z) + \frac{2\,\sigma_w}{r} \right) \kappa_j\, \alpha_{s\,j} \right] \times \left[\sum_{j=1}^{3} \rho_{a\,j}\, \kappa_j \right]^{-1} \right\} \left[p_a + \rho_w\, g(H-z) + \frac{4\,\sigma_w}{3\,r} \right]. \tag{4}$$

The equations for the methane mole fraction originally filling the bubble, and for the mole fractions of the nitrogen and the oxygen, which diffuse in the bubble or from it in the course of floating up.

The first component in the curly brackets in each equation characterises the effect on the molar fraction of the gas in question and the diffusion of the other two gases through the bubble's surface, and the second component characterizes the effect of the variation in external pressure on the intensity of diffusion, which depends on the partial pressure of the gas in the bubble:

$$\frac{d\kappa_j}{dt} = \frac{4.35}{\pi}\sqrt{\frac{w}{r^3}}\left\{\sum_{i=1}^{3}\frac{\kappa_j}{\kappa_i}\left[\alpha_{s\,j}\sqrt{k\,D_j}-\alpha_{s\,i}\sqrt{k\,D_i}\right]\varepsilon_i - \frac{p_a}{p_a+\rho_w\,g(H-z)+\dfrac{2\,\sigma_w}{r}}\times\right.$$
$$\left.\times\sum_{i=1}^{3}\frac{\kappa_j}{\kappa_i}\left[\frac{\alpha_{w\,j}}{\kappa_j}\sqrt{k\,D_j}-\frac{\alpha_{w\,i}}{\kappa_i}\sqrt{k\,D_i}\right]\right\}\left(\sum_{i=1}^{3}\frac{\kappa_j}{\kappa_i}\right)^{-2}. \quad (5)$$

In these formulae, the following notations are used: t and z are the time and the vertical co-ordinate with an origin on the seabed, r and w are the radius of gas bubble and its velocity of floating up, ρ_{aj}, μ_j and κ_j are the density of j-gas inside the bubble under normal atmospheric pressure, its gram-molecular weight and the mole fraction. Then, α_{sj} and α_{wj} are the saturating and real (in seawater) relative volumetric content of j-gas, D_j is the diffusion coefficient of j-gas through the bubble's surface in the seawater without surfactants, k is the coefficient that accounts for the effect of the surfactant film on the diffusion intensity, and H and p_a are the initial depth and the atmospheric pressure. Then, ρ_w and σ_w are the mass density and the capillary constant of the seawater, g is the gravity acceleration, ζ is the drag coefficient and ε_j is the relative part of the bubble surface, through which j-gas diffuses.

Value ε_j depends on the fraction of j-gas in the total gas flux, and the following formula determines it:

$$\varepsilon_j = \frac{\mu_j\sqrt{D_j}\left|(\alpha_{wj}-\alpha_{sj})\right|}{\sum_{i=1}^{3}\mu_i\sqrt{D_i}\left|(\alpha_{wi}-\alpha_{si})\right|}. \quad (6)$$

Initial data concerning the concentration and the solubility of the gases proper to seawater, referenced in [15] and presented in Table 3, were used for the modelling of the gas-bubble dynamic. To take into account the surfactant film forming on the bubble's border and its influence on the bubble's dissolution, the correction to the diffusion coefficient (k = 0.10) was accepted [28]. In the course of modelling, the initial sizes of bubbles (0.5–3.0 mm) and their initial depths (until 250 m) varied according to the results of the acoustic sounding [25,26]. The first goal of modelling was the range of the depths, from which the flowing up of bubbles to the ice cover was possible. The second goal was to estimate the amount of methane in relation to the initial amount that the bubbles were capable of carrying from the seabed to the sea-ice cover.

Table 3. Characteristics of gases and their anticipated concentrations.

Gas	Gramm-Molar Weight, μ_j	Molar Diffusion Coefficient, D_j, m^2/s	Saturating Relative Volume Content, α_{sj}	Relative Volume Content in Sea Water, α_{fj}
Methane	14	0.85×10^{-9}	4.23×10^{-2}	2.09×10^{-5}
Nitrogen	28	1.29×10^{-9}	1.72×10^{-2}	1.20×10^{-2}
Oxygen	32	1.54×10^{-9}	3.61×10^{-2}	0.11×10^{-2}

Figure 5 shows the ranges of depths, from which the bubbles fumed by the bottom sediments or the natural gas deposits are capable of floating up to the ice cover; the bubbles

are not dissolved completely. Figure 6 illustrates the amount of methane that the emerged bubbles are capable of carrying to the lower surface of the ice cover.

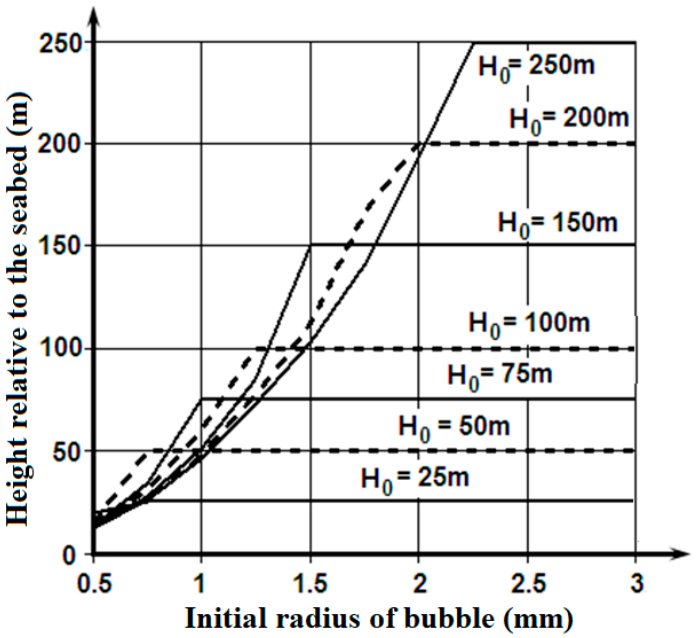

Figure 5. Height relative to the seabed (H) to which methane bubbles with various initial dimensions (R_0) are capable of floating up from the various depths of emission (H_0).

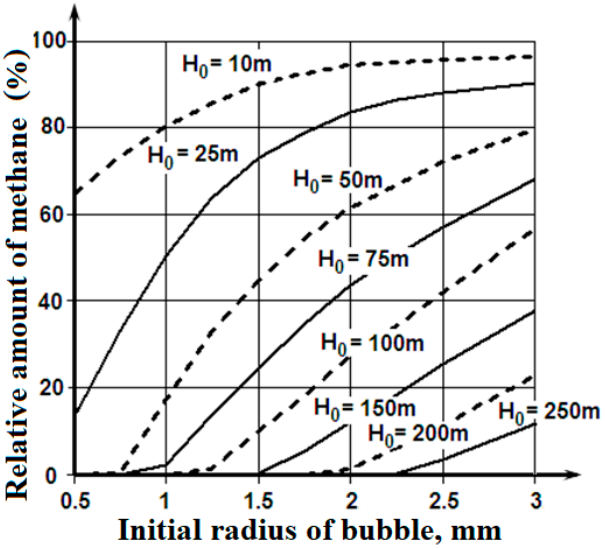

Figure 6. Relative quantities of the initial content of the methane (δQ) that emerging bubbles with various initial dimensions (R_0) are capable of carrying to the lower surface of an ice cover from various depths of emission (H_0).

These materials show that the bubbles fumed by the seabed sediments or the natural gas deposits at depths of 100–150 m, and filled with methane with an initial radius of more than 1.5 mm, are capable of really increasing the porosity on the lower surface of the ice cover. It is a possible explanation of the lower layer of the ice cover porosity, which exceeds values that are connected with the replacement of the gases dissolved in the seawater between the ice crystals.

The considered mechanism can also apply to the deep-water sources of the bubbles containing methane, which form plumes on the marine natural gas fields. In that case,

there is consecutive transformation during the gas bubbles' floating up process: the bubble with methane—the globule of crystalline hydrate of methane [17]. Disintegration of the formation of crystalline hydrate of methane globules of the usual bubbles can occur at depths of 200–150 m. The following process of the gas bubble floating up is similar to the one modelled previously, and the results in Figures 5 and 6 are applicable to it.

6. Conclusions

The problem of sea-ice saturation with gas bubbles has a practical value as the porosity defines the strength of the ice cover. Studies of the mechanisms of the porosity formation process will allow us to predict the strength characteristics of sea-ice cover that will be based on the place of its formation. It would be very interesting to see laboratory experiments based on the controlled variation of air access to the ice samples during freezing.

Research carried out has shown that a porosity increase on the lower border of an ice cover can be the consequence of the capturing of bubbles containing methane formed as a result of the decomposition of seabed sediments, or leaks of methane from marine natural gas deposits. This allows us to assume that ice cover formed in the shallow water areas would have a lesser strength than ice with the same thickness in the deep-water areas. On the other hand, the increased porosity or the concentration of methane in the lower layer of the ice cover can specify the probable existence of seabed deposits of natural gas in the given water area.

The diversity in the shape of the gas cavities in the sea ice indicates that their formation is the result of various physical mechanisms. The study of these mechanisms is of scientific interest and can be used in practical applications. This article discussed the three most obvious mechanisms that are associated with the shape of the gas cavities and with the interaction of the sea ice with the atmosphere and the underlying seawater space. This does not exclude the possibility of the existence of other mechanisms, the search for and study of which are the tasks of further research into the physics of sea ice.

Author Contributions: Conceptualization, V.K.G.; Methodology, V.K.G.; Software, N.Yu.K.; Validation, V.K.G. and N.Yu.K.; Formal analysis, V.K.G. and N.Yu.K.; Investigation, V.K.G. and N.Yu.K.; Writing—original draft, N.Yu.K.; Writing—review & editing, V.K.G.; Visualization, N.Yu.K. All authors have read and agreed to the published version of the manuscript.

Funding: The study of the problem was started in joint project of Saint Petersburg State Marine Technical University (RFBR Grant No. 08-08-92205) and Taiyuan University of Technology (NSFC Grant No. 60811120556), completed and prepared for publication with partially funding by the Ministry of Science and Higher Education of the Russian Federation as part of the World-Class Research Center Program: Advanced Digital Technologies (contract No. 075-15-2022-312 dated 20 April 2022).

Data Availability Statement: Data contained within article are available in a publicly accessible repository.

Conflicts of Interest: The authors declare that this study received funding from RFBR, NSFC and Ministry of Science and Higher Education of the Russian Federation. The funders were not involved in the study design, collection, analysis, interpretation of data, the writing of this article or the decision to submit it for publication.

References

1. Frolova, I.V.; Gavrilo, V.P. (Eds.) *Sea Ice*; Reference book; Gidrometeoizdat: Saint Petersburg, Russia, 1997; p. 402.
2. Shokr, M.E.; Sinha, N.K. Arctic Sea Ice Microstructure Observation Relevant to Microwave Scattering. *Arctic* **1994**, *47*, 265–279. [CrossRef]
3. Wang, Q.; Lu, P.; Leppäranta, M.; Cheng, B.; Zhang, G.; Li, Z. Physical properties of summer sea ice in the Pacific sector of the Arctic during 2008–2018. *J. Geophys. Res. Ocean.* **2020**, *125*, e2020JC016371. [CrossRef]
4. Mellor, M. Mechanical behavior of sea ice. In *The Geophysics of Sea Ice*; NATO ASI Series; Untersteiner, N., Ed.; Springer: Boston, MA, USA, 1986; pp. 165–281. [CrossRef]
5. Tucker, W.B.; Perovich, D.K.; Gow, A.J.; Weeks, W.F.; Drinkwater, M.R. Physical Properties of Sea Ice relevant to Remote Sensing. *Geophys. Monogr.* **1992**, *68*, 9–28.

6. Song, Z.; Hou, L.; Whister, D.; Gao, G. Mesoscopic numerical investigation of dynamic mechanical properties of ice with entrapped air bubbles based on a stochastic sparse distribution mechanism. *Compos. Struct.* **2020**, *236*, 111834. [CrossRef]
7. Shao, K.; Zhen, Z.; Gao, R.; Song, M.; Zhang, L.; Zhang, X. Comparative experimental study of the effect of loading rate on the mechanical properties of bubble and clear ice cubes. *Exp. Therm. Fluid Sci.* **2024**, *159*, 111264. [CrossRef]
8. Shao, K.; Song, M.; Shen, J.; Zhang, X.; Pekai, L. Experimental study on the distribution and growth characteristics of trappeed air bubbles in ice slices at different freezing temperatures. *Appl. Therm. Eng.* **2024**, *244*, 122600. [CrossRef]
9. Malinka, A.; Zege, E.; Heygster, G.; Istomina, E. Reflective properties of white sea ice and snow. *Cryosphere* **2016**, *10*, 2541–2557. [CrossRef]
10. Goncharov, V.K.; Klementieva, N.Y.; Qin, J. Analysis of the problem of saturation of ice with air bubbles. In Proceedings of the 21st International Conference on Port and Ocean Engineering under Arctic Conditions (POAC 2011), Montreal, QC, Canada, 10–14 July 2011; p. 10.
11. Light, B.; Maykut, G.A.; Grenfell, T.C. Effects of temperature on the microstructure of first-year Arctic sea ice. *J. Geophys. Res.* **2003**, *108*, 3051. [CrossRef]
12. Zhang, Y.; Li, Z.; Xiu, Y.; Li, C.; Zhang, B.; Deng, Y. Microstructural Characteristics of Frazil Particles and the Physical Properties of Frazil Ice in the Yellow River, China. *Crystals* **2021**, *11*, 617. [CrossRef]
13. Horne, B.A. Marine Chemistry. In *The Structure of Water and the Chemistry of the Hydrosphere*; Wiley–Interscience: Hoboken, NJ, USA, 1970; p. 198.
14. Maeno, N. *Science about Ice*; Mir: Moscow, Russia, 1998; p. 231.
15. Popov, N.I.; Fedorov, K.N.; Orlov, V.M. *Sea Water*; Reference book; Nauka: Moscow, Russia, 1979; p. 328.
16. Goncharov, V.K. Investigation into bubble contents in the upper ocean from their cavitation manifestation Marine n water flow: Analytical treatment of results. *Oceanology* **1997**, *37*, 465–471.
17. Goncharov, V.K. Modelling of evolution of the bubble plumes arising under leaks of natural gas from deep-water pipeline. In Proceedings of the Twenty-fifth Arctic and Marine Oil Spill Program (AMOP), Technical Seminar, Calgary, AB, Canada, 11–13 June 2002; pp. 45–56.
18. Andersen, D.L. A model for determining sea ice properties. Arctic Sea Ice. In Proceedings of the Conference Conducted by the Division of Earth Sciences and Supported by the Office of Naval Research, Easton, MD, USA, 31 December 1958; pp. 148–152.
19. Nakawo, M. Measurement on air porosity of sea ice. *Ann. Glaciol.* **1983**, *4*, 204–208. [CrossRef]
20. Gavrilo, V.P.; Gaitskhoki, B.Y. The statistics of air inclusions in ice. *Sci. Transl. Jerusalem. Israel.* **1970**, *125*, 128.
21. Backstrom, L.G.E.; Eicken, H. Capacitance probe measurements of brine volume and bulk salinity in first-year sea ice. *Cold Reg. Sci. Technol.* **2006**, *46*, 167–180. [CrossRef]
22. Akulichev, V.A.; Bulanov, V.A.; Klenin, S.S. Acoustical probing of the gas bubbles in the sea space. *Akust. Zhurnal* **1986**, *32*, 289–295.
23. Newman, J.N. *Marine Hydrodynamics*, 40th ed.; The MIT Press: Cambridge, UK, 2017; p. 450.
24. Merewether, R.; Olsson, M.S. Acoustically detected hydrocarbon plumes rising from 2-km depths in Guaymes Basin, Gulf of California. *J. Geophys. Res.* **1985**, *90*, 3075–3085. [CrossRef]
25. Anikiev, V.V.; Obszhirov, A.I. Influence of low temperature hydroterms on the gas composition of the bottom water in the Okhotsk Sea. *Oceanologia* **1993**, *33*, 360–366.
26. Goncharov, V.K.; Klementieva, N.Y. Modelling the dynamics and conditions of sound scattering by gas bubbles floating up from deep water oil and gas deposits. *Acoust. Phys.* **1996**, *42*, 323–328.
27. Sovga, E.E.; Lyubartseva, S.P.; Lyubitsky, A.A. Investigation of methane biogeochemistry and mechanisms of its transport in the Black Sea. *Morskoi Gidrophisicheskii Zhurnal* **2008**, *5*, 40–56.
28. Goncharov, V.K.; Klementieva, N.Y. Investigation of surfactant film influence on solution of a moving bubble in sea water. Izvestya Rossiiskoi Akademii Nauk. *Phys. Atmos. Okeana* **1995**, *31*, 705–712.